New Consistent Model for Ferrite Permeability Tensor with Arbitrary Magnetization State

Philippe Gelin, *Associate Member IEEE*, and Karine Berthou-Pichavant

***Abstract*— Partially magnetized ferrites play an important role in a large class of microwave devices. For instance, when the optimal design of circulators, which operate with ferrite in the low magnetic field region, and other ferrite devices (phase shifters, isolators etc.) are considered, permeability tensor is required for arbitrary magnetization. The existing models do not simultaneously provide all tensor components, and their validity domain is limited. The proposed model provides integral expressions for all permeability tensor components, which can be treated numerically without difficulties. The physical nature of the model enforces the causal aspect that is required when numerical time-domain methods (such as finite-difference time domain (FDTD), transmission-line matrix (TLM), time-domain finite-element method (TDFEM), etc.) are used. Finally, the comparison with measurements or specific cases, which can be treated by available models, demonstrates the validity of the proposed approach.**

I. Introduction

BECAUSE of the wide application of the partially magnetized materials in the microwave devices, the calculation of the permeability tensor components is of great interest. In the saturated state, all magnetic moments are aligned. Consequently, the motion of the magnetization vector leads to the Polder [8] tensor. For a partially magnetized state, the situation is more difficult. This is due to the complexity of the domain configuration (orientation, shape, volume, etc.), the difficulty to evaluate the internal field in each domain, and the interactions between them. The first theory, presented by Rado [1], consists of performing a spatial average of responses produced by all domains in the ferrite. For frequencies above the gyroresonance frequency, Rado has developed a theory which provides a good approximation for the extra-diagonal term κ, but inaccurate values for the diagonal ones ($\mu = \mu_z = 1$). Starting from a coaxial configuration of alternatively magnetized parallel and antiparallel domains, Schlömann [2] developed a theory based upon magnetostatic approximation, which takes into account the interactions between domains of opposite magnetization. In the completely demagnetized state, an average of the three diagonal tensor components yields an accurate value for the isotropic permeability. By using experimental characterization cells, Green and Sandy [3] have measured all the tensor components as a function of the ferrite magnetization state. They deduced empirical forms of the diagonal terms (μ and μ_z) compatible with Schlömann's formula in the completely demagnetized state. In their first paper, Igarashi and Naito [4] presented a formula for the transverse diagonal term in a partially demagnetized state. In a subsequent paper [5], they gave an expression for the longitudinal diagonal term μ_z by using the same approach used by Rado. Unfortunately experimental results must be used to adjust certain parameters used in the model.

In all these approaches, the local permeability in each domain takes a Polder tensor form. In [1] and [2], the internal dc field in each domain is approximated by the magnetocrystalline anisotropy field H_a, whatever the external dc applied field. In [1] and [5], the spatial average is performed by considering noninteracting domains. As a result, it is necessary to adjust parameters involved in the local Polder tensor components to compensate for these approximations.

The present theory is also based on average responses of all randomly oriented domains. Unlike Rado [1], and Igarashi and Naito's [5] theories, this model takes into account the interaction between adjacent domains by considering the demagnetizing and the Polder–Smit effect [6], which may occur between domains. Hence, this model does not require adjustment of quantities such as internal static and dynamic fields.

II. Basic Theory

Ferrites in a completely demagnetized state present an internal structure divided into regions, which are, themselves, divided into domains of parallel and antiparallel magnetization, as shown in Fig. 1. The configuration of the regions (direction, volume, etc.) depends upon the fabrication process and the shape of the material. Whatever the configuration complexity (quasi-random or well organized), the macroscopic magnetization vanishes in the demagnetized state.

In the present model, each region is characterized by ϑ, which is the angle between the direction of magnetization and the Oz direction where the dc magnetic field is applied. First, the response of each region will be established by taking into account (in each domain) the evolution in both magnitude and direction of the internal dc field, and interactions between them. The spatial average of the responses of all regions is then performed. Locally, the motion of the magnetization vector $\vec{M}$ in a domain is governed by Gilbert's equation [7]

$$\frac{d\vec{M}}{dt} = \gamma\vec{M} \times (\vec{H}_i + \vec{h}_d) + \frac{\alpha}{M_s}\vec{M} \times \frac{\vec{M}}{dt} \tag{1}$$

where $\vec{H}_i$ is the internal dc magnetic field, $\vec{h}_d$ is the internal dynamic magnetic field, α is the phenomenological loss term,

Manuscript received August 5, 1996; revised April 25, 1997.

The authors are with LEST Enst de Bretagne U.R.A. CNRS, 29285 Brest Cedex, France.

Publisher Item Identifier S 0018-9480(97)05373-8.

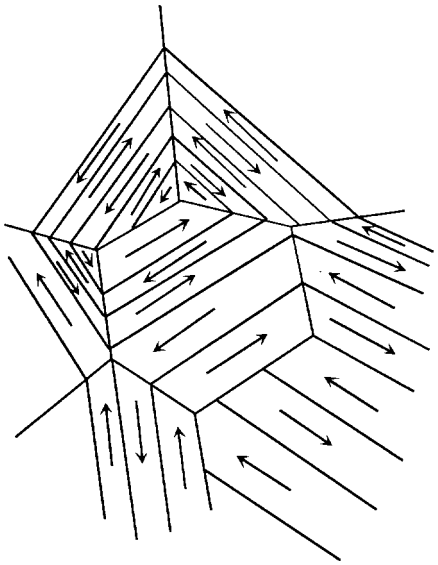

Fig. 1. Example of internal structure of a ferrite in completely demagnetized state.

γ is the gyromagnetic ratio , and M_s is the saturation magnetization. To solve this equation, it is necessary to know $\vec{H}_i$ and $\vec{h}_d$ in each domain.

III. Evaluation of The Dynamical Magnetic F ield:$\vec{h}_d$.

The field $\vec{h}_d$ arises from the RF magnetic field $\vec{h}$ and the demagnetizing field that depends on the shape of the domain. The demagnetizing fields can be explained by the presence of dipolar magnetic charges at the periphery of the domain. Under certain conditions, dipolar charges of two adjacent domains tend to add up and double the value of the demagnetizing field. This phenomenon, which is known as the Polder–Smit effect, couples magnetization vectors of adjacent domains. The first step of the proposed approach is to introduce a directly demagnetizing and Polder–Smit effect in the magnetization vector motion equation (1). The above step can be expressed mathematically by two coupled Gilbert's equations relating two adjacent domains:

$$\frac{d\vec{M}_1}{dt}=\gamma\vec{M}_1\times(\vec{H}_1+\vec{h}-n(\vec{m}_1-\vec{m}_2))+\frac{\alpha}{M_s}\vec{M}_1\times\frac{d\vec{M}_1}{dt}$$
$$\frac{d\vec{M}_2}{dt}=\gamma\vec{M}_2\times(\vec{H}_2+\vec{h}-n(\vec{m}_2-\vec{m}_1))+\frac{\alpha}{M_s}\vec{M}_2\times\frac{d\vec{M}_2}{dt} \quad (2)$$

where

$\vec{M}_1(\vec{M}_2)$	magnetic moment of domain 1 (2);
$\vec{H}_1$ ($\vec{H}_2$	effective dc magnetic field in domain 1 (2);
$\vec{h}$	RF magnetic field;
$\vec{m}_1(\vec{m}_2)$	dynamic part of $\vec{M}_1(\vec{M}_2)$;
n	demagnetizing coefficient depending on the shape of the domains;
$n.(\vec{m}_1-\vec{m}_2)$	represents the dynamic demagnetizing fields (including Polder–Smit effect) in domain 1.

The demagnetizing fields, including a Polder–Smit effect, are maximum when $\vec{m}_1=-\vec{m}_2$ (case where the magnetizations of two adjacent domains are antiparallel). If the material is saturated, $\vec{m}_1=\vec{m}_2$, the internal demagnetizing fields vanishes. In the later case, the demagnetizing dynamic fields distribution depends on the macroscopic shape of the material and, therefore, are included in Maxwell equations and in continuity relations at the interfaces. The demagnetizing coefficient n depends on the shape of the domain ($n=1/2$ for cylindrical shape and $n=1/3$ for spherical shape) and will be discussed later. To solve (2), it is necessary to know the effective dc magnetic field in two adjacent domains.

IV. Evaluation of The Local Effective DC Magnetic Field

The second step consists of evaluating the internal dc field in each domain as a function of the M/M_s ratio when an external dc field is applied. Let $\vec{u}_1$ be the unit vector that defines the equilibrium direction of the local vector $\vec{M}_1$, which is also the direction of the effective dc magnetic field

$$\vec{M}_1=M_s\vec{u}_1+\vec{m}_1 \text{ and } \vec{H}_1=H_1\vec{u}_1. \quad (3)$$

$\vec{H}_1$ is the internal dc field arising from the external applied dc magnetic fields $H_0.\vec{k}$, the macroscopic demagnetizing fields $N_z.M.\vec{k}$, the magnetocrystalline anisotropy field $H_a.\vec{v}$, and the dipolar field $\vec{H}_{\text{dip}}$ (the exchange fields are neglected). Hence, this is written as follows:

$$H_1.\vec{u}_1=H_a.\vec{v}+H_0.\vec{k}-N_z.M.\vec{k}+H_{dip}.\vec{k}=H_a.\vec{v}+H_s.\vec{k} \quad (4)$$

where

$\vec{v}$	randomly oriented unit vector (all the directions are equiprobables for the anisotropy field H_a);
$\vec{H}_0$	applied external dc magnetic field along the Oz axis;
N_z	macroscopic demagnetizing coefficient along the Oz axis depending on the shape of the sample;
M	macroscopic magnetization and $N_z.M$macroscopic demagnetizing field, which appears along Oz;
H_{dip}	average magnetic field created by all magnetic moments into the considered domain. Hence, it also points along Oz;
H_s	total dc magnetic fields along Oz.

The vectors $\vec{u}_1$ and $\vec{v}$ are expressed in the Cartesian system $(\vec{i},\vec{j},\vec{k})$ as

$$\vec{u}_1=\vec{i}.\sin\theta_1.\cos\Phi_1+\vec{j}.\sin\theta_1.\sin\Phi_1+\vec{k}.\cos\theta_1 \quad (5)$$
$$\vec{v}=\vec{i}.\sin\vartheta.\cos\phi+\vec{j}.\sin\vartheta.\sin\phi+\vec{k}.\cos\vartheta. \quad (6)$$

By substituting (5) and (6) into (4), one obtains $\vec{u}_1$ shown in (7) at the bottom of the following page. Therefore, according to (5) the angles Φ, ϕ, θ_1, ϑ are related by

$$\cos\theta_1=\frac{H_a.\cos\vartheta+H_s}{\sqrt{H_a^2+2H_a.H_s.\cos\vartheta+H_s^2}}$$
$$\sin\theta_1=\frac{H_a.\sin\vartheta}{\sqrt{H_a^2+2H_a.H_s.\cos\vartheta+H_s^2}};\phi=\Phi_1. \quad (8)$$

If H_{dip} and $N_z.M$ are assumed uniform in the whole sample, the quantity H_s can be related to the ratio M/M_s by expressing the average of the $\vec{u}_1$ projection on (Oz) as follows:

$$< \cos\theta >= \frac{M}{M_s} = \frac{1}{4.\pi} \int_0^{2\pi} \int_0^{\pi} \sin\vartheta . \cos\theta_1 . d\vartheta . d\phi.$$

Thus, using (8), one obtains the following relations:

$$\begin{cases} H_s = \frac{H_a}{\sqrt{3.(1-<\cos\theta>)}}, & \text{for } < \cos\theta > \geq 2/3 \\ H_s = \frac{3H_a}{2} < \cos\theta >, & \text{for } < \cos\theta > \leq 2/3. \end{cases} \quad (9)$$

These relations show that the magnitude of the internal dc field is of the same order of the anisotopy field H_a up to about $M/M_s = 2/3$.

A. Local Internal dc Fields in Adjacent Domains

If $\vec{H}_a$ is the magnetocrystalline field in domain 1, $-\vec{H}_a$ is the one in the adjoining domain 2. Thus, $\Phi_1 = \phi$ and $\Phi_2 = \phi + \pi$. Consequently, the magnetization and the magnetic field in each domain is given by

$$\begin{aligned} \vec{M}_1 &= M_s \vec{u}_1 + \vec{m}_1 \quad \vec{H}_1 = H_1 \vec{u}_1 \\ \vec{M}_2 &= M_s \vec{u}_2 + \vec{m}_2 \quad \vec{H}_2 = H_2 \vec{u}_2 \end{aligned} \quad (10)$$

with

$$\begin{aligned} \vec{u}_1 &= \sin\theta_1 . \cos\phi . \vec{i} + \sin\theta_1 . \sin\phi . \vec{j} + \cos\theta_1 . \vec{k} \\ \vec{u}_2 &= -\sin\theta_2 . \cos\phi . \vec{i} - \sin\theta_2 . \sin\phi . \vec{j} + \cos\theta_2 . \vec{k} \end{aligned} \quad (11)$$

and according to (7) and (8)

$$\begin{cases} H_1 = \sqrt{H_a^2 + 2H_a . H_s . \cos\vartheta + H_s^2} \\ H_2 = \sqrt{H_a^2 - 2H_a . H_s . \cos\vartheta + H_s^2} \\ \sin\theta_1 = H_a . \sin\vartheta / H_1 \\ \sin\theta_2 = H_a . \sin\vartheta / H_2 \\ \cos\theta_1 = (H_s + H_a . \cos\vartheta)/H_1 \\ \cos\theta_2 = (H_s - H_a . \cos\vartheta)/H_2. \end{cases} \quad (12)$$

Fig. 2 illustrates the evolution of the dc internal fields in adjacent domains for different regions in the ferrite material. From a physical point of view, this model does not represent the reality. Actually, one knows that the volume of the domain increases or decreases depending on the orientation of its magnetization vector with respect to the applied dc magnetic field, before the rotation of the magnetization vector occurs.

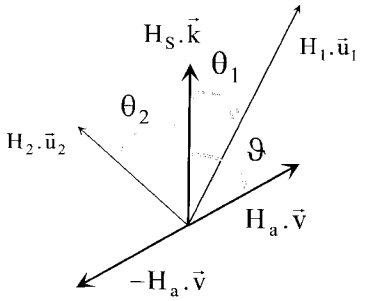

Fig. 2. Calculation of the internal field in each domain.

V. Solutions of the Coupled Gilbert's Differential Equations

Since the internal field in each domain is known, one can solve the coupled Gilbert's differential equations (2). By substituting (3) into (2), and using small signal approximation, the coupled Gilbert's equations become

$$\begin{aligned} j\omega . \vec{m}_1 =& \gamma . M_s \vec{u}_1 \times (\vec{h} - n . \vec{m}_1 + n . \vec{m}_2) \\ &+ \gamma . \vec{m}_1 \times H_1 \vec{u}_1 + j\omega\alpha . \vec{u}_1 \times \vec{m}_1 \\ j\omega . \vec{m}_2 =& \gamma . M_s \vec{u}_2 \times (\vec{h} - n . \vec{m}_2 + n . \vec{m}_1) \\ &+ \gamma . \vec{m}_2 \times H_2 \vec{u}_2 + j\omega\alpha . \vec{u}_2 \times \vec{m}_2. \end{aligned} \quad (13)$$

First, (13) is solved in the local coordinate systems $(\vec{u}_i, \vec{\theta}_i, \vec{\phi}_i)$ (see Appendix I). These equations are then decoupled before writing them in the Cartesian coordinate system (see Appendix II). Finally, performing a simple integration over ϕ (see Appendix III), one obtains all components of the permeability tensor shown in (14), at the bottom of the page. These expressions are easily computed using (9), (12), and factors $A(\vartheta)$, $B(\vartheta)$, $C(\vartheta)$, $D(\vartheta)$, $E(\vartheta)$, and $F(\vartheta)$, whose analytical expression is given in (AIII-8) (Appendix III).

VI. Results

In this section, the present model is compared to other theoretical approaches available in the literature [1]–[3] and with the published measurements in [9]. The first comparison concerns the demagnetized state, for which Schlömann's formula is a good approximation. This case corresponds to $Hs = 0$. Equation (14) then takes the following analytical

$$\vec{u}_1 = \frac{H_a . \sin\vartheta . \cos\phi . \vec{i} + H_a . \sin\vartheta . \sin\phi . \vec{j} + (H_a . \cos\vartheta + H_s) . \vec{k}}{\sqrt{H_a^2 . \sin^2\vartheta + (H_a . \cos\vartheta + H_s)^2}} \quad (7)$$

$$\begin{cases} < \mu >= 1 + \frac{1}{4} \int_0^{\pi} (B(\vartheta)\cos^2\theta_1 + D(\vartheta) + C(\vartheta)\sin\theta_1\cos\theta_1)\sin\vartheta . d\vartheta \\ < \kappa >= \frac{j}{4} \int_0^{\pi} (A(\vartheta)\cos\theta_1 - F(\vartheta)\sin\theta_1 - E(\vartheta)\cos\theta_1)\sin\vartheta . d\vartheta \\ < \mu_z >= 1 + \frac{1}{2} \int_0^{\pi} (B(\vartheta)\sin^2\theta_1 - C(\vartheta)\sin\theta_1\cos\theta_1)\sin\vartheta . d\vartheta \end{cases} \quad (14)$$

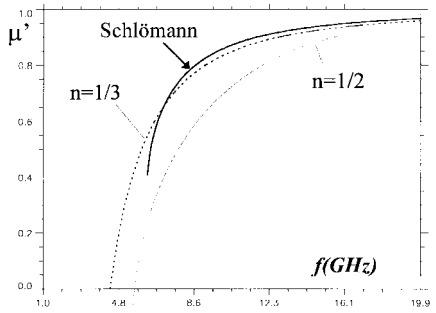

Fig. 3. Real part of μ of completely demagnetized ferrite as a function of frequency ($Ms = 159.15$ kA/m). Comparison with Schlömann's formula.

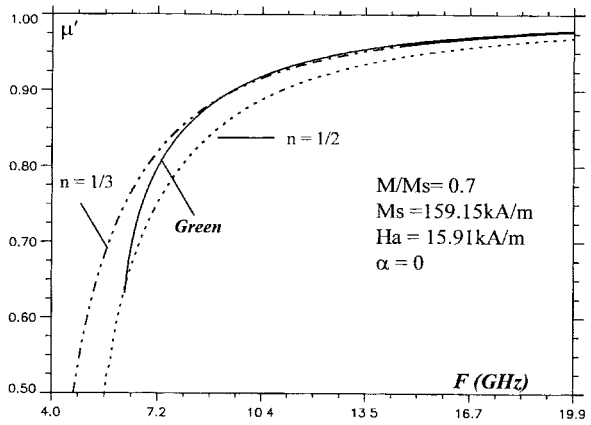

Fig. 4. Real part of μ of partially magnetized ferrite as a function of frequency ($Ms = 159.15$ kA/m). Comparison with Green and Sandy's formulas.

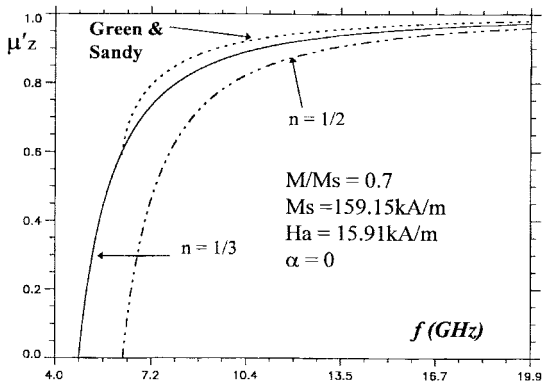

Fig. 5. Real part of parallel component of partially magnetized ferrite as a function of frequency ($Ms = 159.15$ kA/m). Comparison with Green and Sandy's formulas.

form:

$$<\mu>=<\mu_z> = \frac{1}{3}+\frac{2}{3}\left[\frac{(\omega_a - j\omega\alpha+\omega_m)(\omega_a - j\omega\alpha+2n.\omega_m)-\omega^2}{(\omega_a - j\omega\alpha)(\omega_a - j\omega\alpha+2n.\omega_m)-\omega^2}\right],$$
$$\text{and } <\kappa>=0$$

In Fig. 3, the isotropic permeability is compared to Schlö mann's formula for $n = 1/2$ and $n = 1/3$. A good accordance is observed within the validity limits of Schlömann's theory. The value $n = 1/3$, which corresponds to an averaging

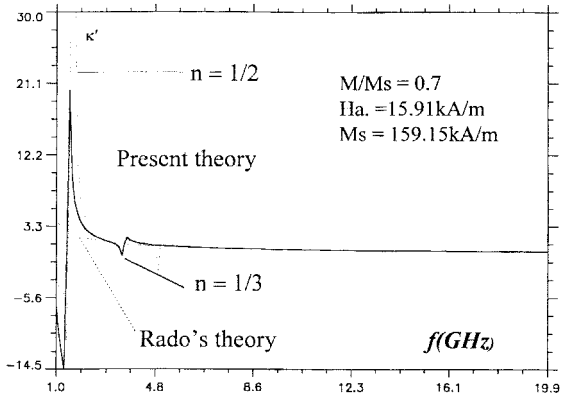

Fig. 6. Real part of κ as a function of frequency ($Ms = 159.15$ kA/m). Comparison with Rado's formula (partially magnetized ferrite).

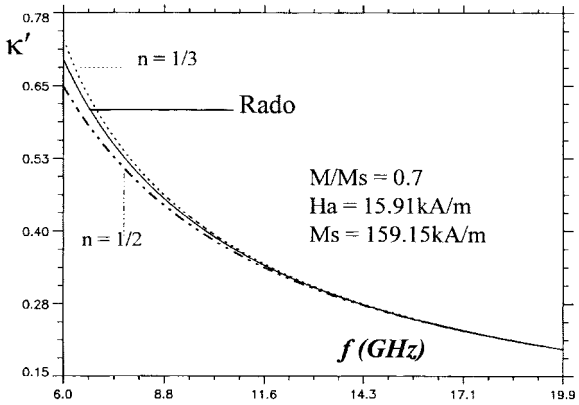

Fig. 7. Real part of κ as a function of frequency ($Ms = 159.15$ kA/m). Comparison with Rado's formula (partially magnetized ferrite).

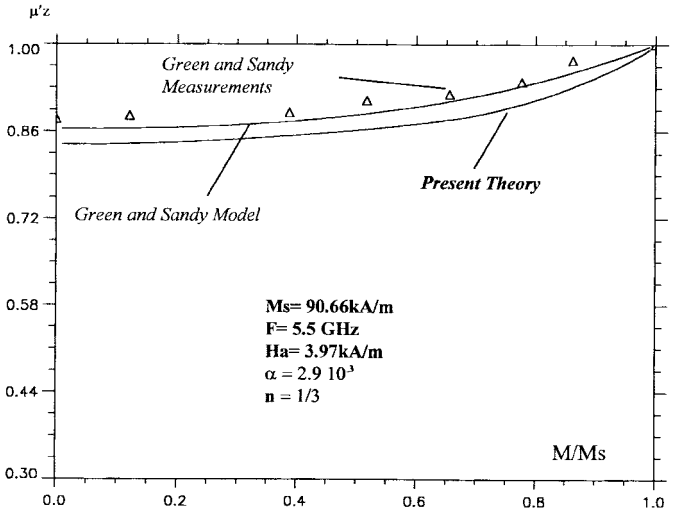

Fig. 8. Real part of μz as a function of M/Ms. Comparison with Green and Sandy's formulas and measurements.

spherical shape of domains, seems to better fit Schlömann's formula. Note that the present model is not limited to low frequencies, for which losses are important.

Figs. 4 and 5 show an example of comparison with Green and Sandy's formulas for the diagonal elements μ' and μ'_z. These curves, established for $M/M_s = 0.7$, confirm a better

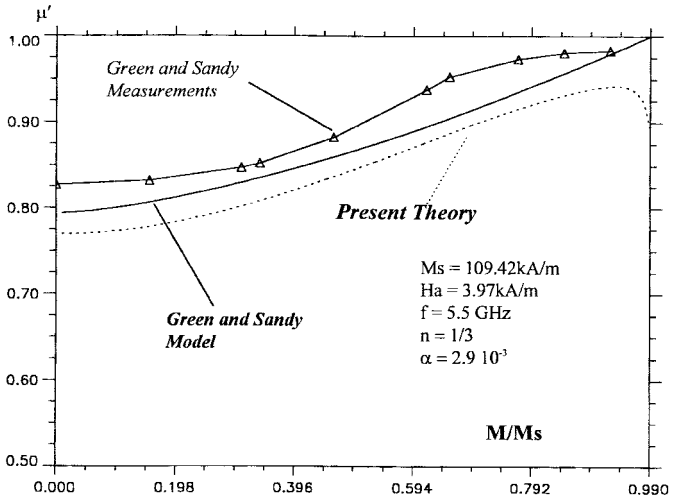

Fig. 9. Real part of μ as a function of M/Ms. Comparison with Green and Sandy's formulas and measurements.

behavior for the value $n = 1/3$. In the low-frequency region (Fig. 6), where Rado's model assumptions are not verified, there is a resonance phenomenon. In the region where Rado's theory is valid, the agreement is quite good (Fig. 7). As noticed by several authors, the Polder–Smit effect does not have significant influence on κ'. This explains the weak difference between the curve $n = 1/2$ and $n = 1/3$. Figs. 8 and 9 illustrate the good prediction provided by the proposed model regarding diagonal elements when compared with measurements published in [9]. This comparison is shown for the optimum value of the demagnetizing factor $n = 1/3$. Note that the analytical expressions in [4] are closer to the experimental measured points. The reason is that this expression was obtained from a curve fitting of these points.

To compare this model with the Polder tensor, it is necessary to know the correspondence between M/M_s and H_0 (Polder tensor). Here, H_0 takes the value of the internal field H_s defined by (9). For example, with $M/Ms = 0.999$ and $H_a = 15.91$ kA/m, the internal field H_s is 290.58 kA/m. Figs. 10 and 11 show that for a given value of the damping term α, the present model provides lower amplitude for the real part of μ and κ because it takes the dispersion of magnetocrystalline anisotropy fields into account. The comparison is presented over the small frequency range of the gyromagnetic resonance. Out of this range the curves are exactly the same. On the other hand, the imaginary parts, which are directly related to the coefficient α, are not modified significantly (see Fig. 12).

The last curves (Figs. 13 and 14) illustrate the behavior of the diagonal term μ as a function of frequency for various states of magnetization. For nonsaturated medium, losses are important in the low-frequency region (low field losses) and decrease with the M/Ms ratio. When saturation is reached, losses only appears at Larmor frequency ($\omega_0 = \gamma.Hs$).

VII. Conclusion

Permeability tensor components are, for the first time, derived from a self-consistent model. Hence, the causality which is required for using time-domain electromagnetic (EM) methods is achieved. Furthermore, this model allows one to describe the permeability tensor for arbitrary magnetization state (demagnetized partially or totally magnetized). It is also found that the model is in accordance with previous theories within their validity limits and with measurements published in the literature. In addition, the proposed model can be improved by coupling it with a prediction model of the hysteresis curve. Such a model [10] allows one to obtain M/M_s behavior as

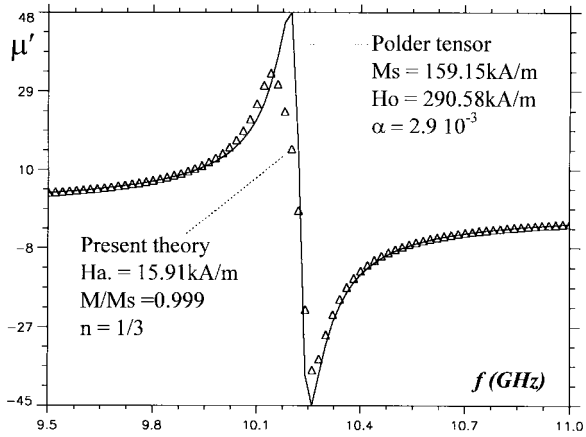

Fig. 10. Real part of μ as a function of frequency ($Ms = 159.15$ kA/m). Comparison with Polder tensor (saturated ferrite).

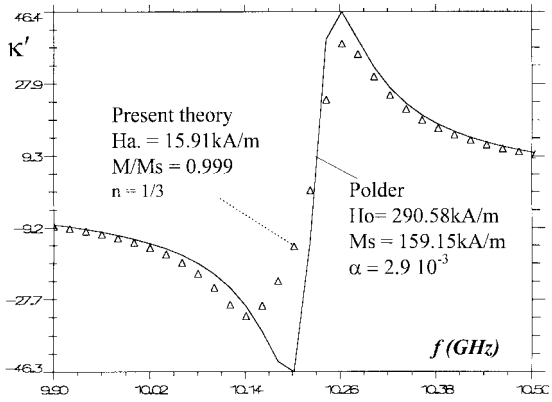

Fig. 11. Real part of κ as a function of frequency ($Ms = 159.15$ kA/m Comparison with Polder tensor (saturated ferrite).

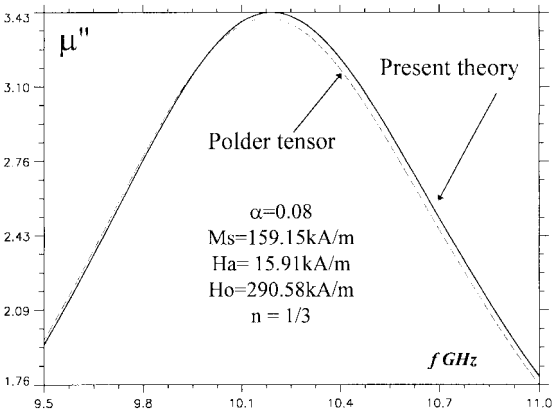

Fig. 12. Imaginary part of μ as a function of frequency ($Ms = 159.15$ kA/m). Comparison with Polder tensor (saturated ferrite).

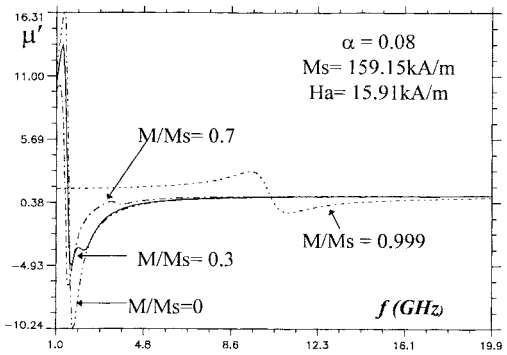

Fig. 13. Real part of μ of ferrite as a function of frequency for different M/Ms ratios.

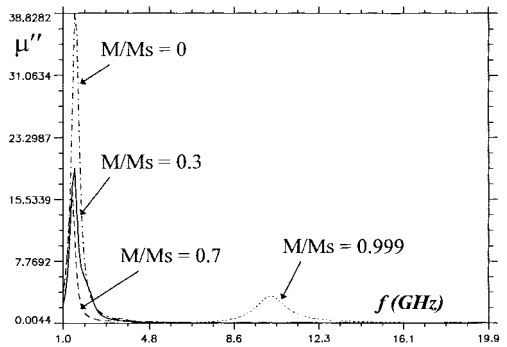

Fig. 14. Imaginary part of μ of ferrite as a function of frequency for different M/Ms ratios.

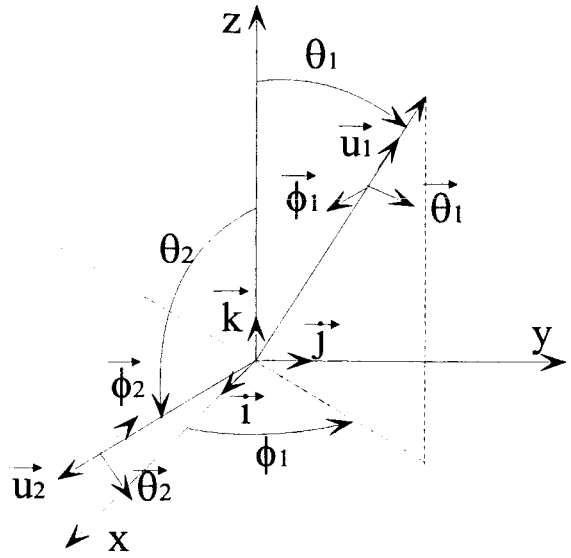

Fig. 15. Local coordinate systems.

a function of the field applied Ho. Consequently, coupled models should be able to reproduce a second-order hysteresis effect observed experimentally by Green and Sandy.

APPENDIX I

A. Local Coordinate Systems

See Fig. 15.

B. Relation Between Basis Vectors of the Coordinates Systems

$$\begin{aligned}
\vec{u}_1 &= \sin\theta_1\cos\phi\vec{i} + \sin\theta_1\sin\phi\vec{j} + \cos\theta_1\vec{k}\\
\vec{\phi}_1 &= \sin\phi\vec{i} - \cos\phi\vec{j} = \vec{\phi}\\
\vec{\theta}_1 &= \cos\theta_1\cos\phi\vec{i} + \cos\theta_1\sin\phi\vec{j} - \sin\theta_1\vec{k}\\
\vec{u}_2 &= -\sin\theta_2\cos\phi\vec{i} - \sin\theta_2\sin\phi\vec{j} + \cos\theta_2\vec{k}\\
\vec{\phi}_2 &= -\sin\phi\vec{i} + \cos\phi\vec{j} = -\vec{\phi}\\
\vec{\theta}_2 &= -\cos\theta_2\cos\phi\vec{i} - \cos\theta_2\sin\phi\vec{j} - \sin\theta_2\vec{k} \quad \text{(AI-1)}\\
\vec{u}_2 &= \cos(\theta_2+\theta_1)\vec{u}_1 - \sin(\theta_2+\theta_1)\vec{\theta}_1\\
\vec{\phi}_2 &= -\vec{\phi}_1 = -\vec{\phi}\\
\vec{\theta}_2 &= -\sin(\theta_1+\theta_2)\vec{u}_1 - \cos(\theta_2+\theta_1)\vec{\theta}_1. \quad \text{(AI-2)}
\end{aligned}$$

C. Resolution of (13) in the Local Coordinate System

$$\vec{m}_i = m_{ui}.\vec{u}_i + m_{\theta i}.\vec{\theta}_i + m_{\phi i}.\vec{\phi}_i, \qquad i \in \{1,2\}. \quad \text{(AI-3)}$$

According to (13), (AI-3), and using the vectorial relations between the basis vectors of the two local coordinate systems, one obtains an expression of the following three components of the dynamic magnetization vector:

$$\begin{aligned}
m_{\theta i} &= j\frac{\omega.\omega_m(h_{\phi i} - n.m_{\phi i} + n.m^i_{\phi k})}{(\omega_i - j\omega\alpha)^2 - \omega^2}\\
&\quad + \frac{\omega_m.(\omega_i - j\omega\alpha)(h_{\theta i} - n.m_{\theta i} + n.m^i_{\theta k})}{(\omega_i - j\omega\alpha)^2 - \omega^2}\\
m_{\phi i} &= -j\frac{\omega.\omega_m(h_{\theta i} - n.m_{\theta i} + n.m^i_{\theta k})}{(\omega_i - j\omega\alpha)^2 - \omega^2}\\
&\quad + \frac{\omega_m.(\omega_i - j\omega\alpha)(h_{\phi i} - n.m_{\phi i} + n.m^i_{\phi k})}{(\omega_i - j\omega\alpha)^2 - \omega^2}\\
m_{ui} &= 0 \quad \text{(AI-4)}
\end{aligned}$$

with

$$\omega_i = \gamma.H_i \quad \text{and} \quad \omega_m = \gamma.M_s. \quad \text{(AI-5)}$$

In (AI-4), $m^i_{\phi k}$ and $m^i_{\theta k}$ are the components of $\vec{m}_k$ written in the local coordinate system (i).

APPENDIX II: DECOUPLING OF (AI-4)

A. Expression of the m Components in the Two Local Systems

Expressing $\vec{m}_2$ in the two local coordinate systems

$$\begin{aligned}
\vec{m}_2(\theta,\phi) &= m_{u2}.\vec{u}_2 + m_{\phi 2}.\vec{\phi}_2 + m_{\theta 2}.\vec{\theta}_2\\
&= m^1_{u2}.\vec{u}_1 + m^1_{\phi 2}.\vec{\phi}_1 + m^1_{\theta 2}.\vec{\theta}_1
\end{aligned}$$

and using $m_{u2} = 0$ (AI-4), one has

$$\begin{aligned}
m^1_{u2} &= -m_{\theta 2}.\sin(\theta_1+\theta_2)\\
m^1_{\phi 2} &= -m_{\phi 2}\\
m^1_{\theta 2} &= -m_{\theta 2}.\cos(\theta_2+\theta_1). \quad \text{(AII-1)}
\end{aligned}$$

Letting $\delta = \cos(\theta_1 + \theta_2), \lambda = \sin(\theta_1 + \theta_2), \Omega_i = \omega_i - j\omega\alpha + n\omega_m$, the following relations are obtained:

$$\begin{aligned}(\Omega_1^2 - \omega^2)m_{\theta 1} &= j\omega.\omega_m h_{\phi 1} + \omega_m \Omega_1 h_{\theta 1} \\ &\quad - j\omega.\omega_m n m_{\phi 2} - \omega_m \Omega_1 n\delta m_{\theta 2} \\ (\Omega_1^2 - \omega^2)m_{\phi 1} &= \omega_m \Omega_1 h_{\phi 1} - j\omega.\omega_m h_{\theta 1} \\ &\quad + j\omega.\omega_m n\delta m_{\theta 2} - \omega_m \Omega_1 n m_{\phi 2} \quad \text{(AII-2)} \\ (\Omega_2^2 - \omega^2)m_{\theta 2} &= j\omega.\omega_m h_{\phi 2} + \omega_m \Omega_2 h_{\theta 2} \\ &\quad - j\omega.\omega_m n m_{\phi 1} - \omega_m \Omega_2 n\delta m_{\theta 1} \\ (\Omega_2^2 - \omega^2)m_{\phi 2} &= \omega_m \Omega_2 h_{\phi 2} - j\omega.\omega_m h_{\theta 2} \\ &\quad + j\omega.\omega_m n\delta m_{\theta 1} - \omega_m \Omega_2 n m_{\phi 1}. \quad \text{(AII-3)}\end{aligned}$$

Now the problem is to eliminate all terms with subscript 2 to obtain $m_{\theta 1}$ and $m_{\phi 1}$ versus $h_{\phi 1}$ and $h_{\theta 1}$. The first step consists of including the expressions of $m_{\theta 2}$ and $m_{\phi 2}$(AII-3) into (AII-2). As a result, only two equations are obtained, linking $m_{\theta 1}$, $m_{\phi 1}$, $h_{\phi 1}$, $h_{\phi 2}$, $h_{\theta 1}$, $h_{\theta 2}$. It is then necessary to write $h_{\theta 2}$ and $h_{\phi 2}$ as a function of $h_{u1}, h_{\theta 1}, h_{\phi 1}$. Noticing that the wavelength is several orders greater than the dimensions of the domains, h can be considered the same in two adjoining domains. Thus

$$\begin{aligned}h_{u2}.\vec{u}_2 + h_{\phi 2}.\vec{\phi}_2 + h_{\theta 2}.\vec{\theta}_2 &= h_{u1}.\vec{u}_1 + h_{\phi 1}.\vec{\phi}_1 + h_{\theta 1}.\vec{\theta}_1 \\ h_{u2} &= h_{u1}.\delta - h_{\theta 1}.\lambda \\ h_{\phi 2} &= -h_{\phi 1} \\ h_{\theta 2} &= -h_{u1}.\lambda - h_{\theta 1}.\delta. \quad \text{(AII-4)}\end{aligned}$$

Hence, the following equations are obtained:

$$\begin{aligned}&\left[(\Omega_1^2 - \omega^2)(\Omega_2^2 - \omega^2) - \omega^2\omega_m^2 n^2\delta - \omega_m^2 \Omega_1 n^2 \delta^2 \Omega_2\right].m_{\theta 1} \\ &= j\omega\omega_m^2 n^2(\Omega_2 + \Omega_1\delta).m_{\phi 1} + j\omega.\omega_m(\Omega_2^2 - \omega^2 + \omega_m n\Omega_2 \\ &\quad + \omega_m \Omega_1 n\delta).h_{\phi 1} + \omega_m(\Omega_1\Omega_2^2 - \omega^2\Omega_1 + \omega^2\omega_m n\delta \\ &\quad + \omega_m \Omega_1 n\delta^2\Omega_2).h_{\theta 1} + \omega_m^2 n\lambda(\omega^2 + \Omega_1\Omega_2\delta).h_{u1} \quad \text{(AII-5)}\end{aligned}$$

$$\begin{aligned}&\left[(\Omega_1^2 - \omega^2)(\Omega_2^2 - \omega^2) - \omega^2\omega_m^2 n^2\delta - \omega_m^2 \Omega_1 n^2 \Omega_2\right].m_{\phi 1} \\ &= -j\omega\omega_m^2 n^2\delta(\Omega_1 + \delta\Omega_2).m_{\theta 1} + \omega_m(\Omega_1\Omega_2^2 - \omega^2\Omega_1 \\ &\quad + \omega^2\omega_m n\delta + \omega_m\Omega_1 n\Omega_2).h_{\phi 1} - j\omega.\omega_m(\Omega_2^2 - \omega^2 \\ &\quad + \omega_m n\delta^2\Omega_2 + \omega_m\Omega_1 n\delta).h_{\theta 1} - j\omega\omega_m^2 n\lambda(\delta\Omega_2 + \Omega_1).h_{u1}. \quad \text{(AII-6)}\end{aligned}$$

Finally, by decoupling the previous equations, the magnetization vector $\vec{m}$ is related to the microwave magnetic field $\vec{h}$. The result is

$$\begin{aligned}m_{\theta 1} &= A(\vartheta).h_{\phi 1} + B(\vartheta).h_{\theta 1} + C(\vartheta).h_{u1} \\ m_{\phi 1} &= D(\vartheta).h_{\phi 1} + E(\vartheta).h_{\theta 1} + F(\vartheta).h_{u1} \quad \text{(AII-7)}\end{aligned}$$

with $A(\vartheta)$, $B(\vartheta)$, $C(\vartheta)$, $D(\vartheta)$, $E(\vartheta)$, $F(\vartheta)$, and Den shown in (AII-8) at the bottom of the page. Note that the transverse components of m depend on the radial components of h due to the coupling between domains.

B. Relations Between m and h in the Cartesian System

Equation (AII-7) represents the motion of a magnetization vector in domain 1 of the region, where the magnetocrystalline field is defined by (ϑ, ϕ). Before adding the contribution of all domains, one should transform (AII-7) back to the Cartesian coordinate system $(\vec{i}, \vec{j}, \vec{k})$ as follows:

$$\vec{m} = m_x\vec{i} + m_y\vec{j} + m_z\vec{k} = m_{\theta 1}\vec{\theta}_1 + m_{\phi 1}\vec{\phi}_1 \quad \text{(AII-9)}$$

$$\begin{aligned}h_{\theta 1} &= h_x\cos\theta_1\cos\phi + h_y\cos\theta_1\sin\phi - h_z\sin\theta_1 \\ h_{\phi 1} &= h_x\sin\phi - h_y\cos\phi \\ h_{u1} &= h_x\sin\theta_1\cos\phi + h_y\sin\theta_1\sin\phi + h_z\cos\theta_1. \quad \text{(AII-10)}\end{aligned}$$

$$\begin{cases}A(\vartheta) = j\omega.\omega_m\left[\Omega_2^2 - \omega^2 + \omega_m n.(\Omega_2 + \Omega_1\delta) + \omega_m^2 n^2\delta\right]/Den \\ B(\vartheta) = \left[-\omega_m^4 n^3\delta^2 + \omega_m\Omega_1(\Omega_2^2 - \omega^2) - \omega_m^3 n^2\Omega_2 + \omega_m^2 n.\delta(\omega^2 + \Omega_1\Omega_2\delta)\right]/Den \\ C(\vartheta) = \omega_m^2 n.\lambda(\omega^2 + \Omega_1\Omega_2\delta - \omega_m^2 n^2\delta)/Den \\ D(\vartheta) = \left[-\omega_m^4 n^3\delta^2 + \omega_m\Omega_1(\Omega_2^2 - \omega^2) - n^2\omega_m^3\delta^2\Omega_2 + n.\omega_m^2(\omega^2\delta + \Omega_1\Omega_2)\right]/Den \\ E(\vartheta) = -j\omega.\omega_m\left[\Omega_2^2 - \omega^2 + \omega_m n.\delta(\Omega_1 + n.\Omega_2) + \omega_m^2 n^2\delta\right]/Den \\ F(\vartheta) = -j\omega\omega_m^2 n.\lambda(\Omega_1 + \delta\Omega_2)/Den \\ \text{Den} = (\Omega_1^2 - \omega^2)(\Omega_2^2 - \omega^2) - n^2\omega_m^2(2\omega^2\delta + \Omega_1\Omega_2\delta^2 + \Omega_1\Omega_2) + n^4\omega_m^4\delta^2 \\ \lambda = \sin(\theta_1 + \theta_2) \qquad \delta = \cos(\theta_1 + \theta_2) \\ \Omega_i = \omega_i - j\omega\alpha + n\omega_m \qquad \omega_i = \gamma.H_i \qquad \omega_m = \gamma.M_s\end{cases} \quad \text{(AII-8)}$$

$$\begin{aligned}\overline{m_x} &= (B(\vartheta)\cos\theta_1^2 + D(\vartheta) + C(\vartheta)\sin\theta_1\cos\theta_1)\pi.h_x + (F(\vartheta)\sin\theta_1 + E(\vartheta)\cos\theta_1 - A(\vartheta)\cos\theta_1)\pi.h_y \\ \overline{m_y} &= (B(\vartheta)\cos\theta_1^2 + D(\vartheta) + C(\vartheta)\sin\theta_1\cos\theta_1)\pi.h_y - (F(\vartheta)\sin\theta_1 + E(\vartheta)\cos\theta_1 - A(\vartheta)\cos\theta_1)\pi.h_x \\ \overline{m_z} &= (B(\vartheta)\sin\theta_1^2 - C(\vartheta)\cos\theta_1\sin\theta_1)2\pi.h_z \quad \text{(AIII-1)}\end{aligned}$$

According to (AII-7), (AII-9), and (AII-10), one writes

$$\begin{aligned} m_x = {} & (A(\vartheta)\cos\theta_1\cos\phi + D(\vartheta)\sin\phi) \\ & \cdot (h_x\sin\phi - h_y\cos\phi) \\ & + (B(\vartheta)\cos\theta_1\cos\phi + E(\vartheta)\sin\phi) \\ & \cdot (h_x\cos\theta_1\cos\phi + h_y\cos\theta_1\sin\phi - h_z\sin\theta_1) \\ & + (C(\vartheta)\cos\theta_1\cos\phi + F(\vartheta)\sin\phi) \\ & \cdot (h_x\sin\theta_1\cos\phi + h_y\sin\theta_1\sin\phi + h_z\cos\theta_1) \end{aligned} \tag{AII-11}$$

$$\begin{aligned} m_y = {} & (A(\vartheta)\cos\theta_1\sin\phi - D(\vartheta)\cos\phi) \\ & \cdot (h_x\sin\phi - h_y\cos\phi) \\ & + (B(\vartheta)\cos\theta_1\sin\phi - E(\vartheta)\cos\phi) \\ & \cdot (h_x\cos\theta_1\cos\phi + h_y\cos\theta_1\sin\phi - h_z\sin\theta_1) \\ & + (C(\vartheta)\cos\theta_1\sin\phi - F(\vartheta)\cos\phi) \\ & \cdot (h_x\sin\theta_1\cos\phi + h_y\sin\theta_1\sin\phi + h_z\cos\theta_1) \end{aligned} \tag{AII-12}$$

$$\begin{aligned} m_z = {} & -A(\vartheta)\sin\theta_1(h_x\sin\phi - h_y\cos\phi) - B(\vartheta)\sin\theta_1 \\ & \cdot (h_x\cos\theta_1\cos\phi + h_y\cos\theta_1\sin\phi - h_z\sin\theta_1) - C(\vartheta) \\ & \cdot \sin\theta_1(h_x\sin\theta_1\cos\phi + h_y\sin\theta_1\sin\phi + h_z\cos\theta_1). \end{aligned} \tag{AII-13}$$

Equations (AII-11)–(AII-13) represent the response of a domain in a region characterized by the angles (ϑ, ϕ). To perform the response of the material, it is now necessary to sum up all the couples $(\vartheta,\ \phi)$.

APPENDIX III

A. Spatial Average of Responses

The effective magnetization vector is obtained by a spatial average of the responses

$$< m_\xi(\vartheta,\phi) >= \frac{1}{4.\pi}\int_0^{2\pi}\int_0^{\pi} m_\xi(\vartheta,\phi).\sin\vartheta.d\vartheta.d\phi$$

where $\xi \in \{x, y, z\}$. First, an integration is performed over ϕ, which yields the average value

$$\overline{m_\xi(\vartheta,\phi)} = \int_0^{2\pi} m_\xi(\vartheta,\phi).d\phi.$$

Terms depending on $\sin\phi$, $\cos\phi$, and $\sin\phi.\cos\phi$ vanish, while the quadratic and constant terms after integration give π and 2π. As a result, (AII-10)–(AII-12) reduces to (AIII-1), shown at the bottom of the previous page. Then the average components of the magnetization vector are computed as follows:

$$< m_\xi(\vartheta,\Phi) >= \frac{1}{4.\pi}\int_0^{\pi} \overline{m_\xi(\vartheta,\phi)}.\sin\vartheta.d\vartheta. \tag{AIII-2}$$

The components of the permeability tensor are obtained from

$$\begin{aligned} < m_x > &= < \mu > .h_x + j < \kappa > .h_y \\ < m_y > &= < \mu > .h_y - j < \kappa > .h_x \\ < m_z > &= < \mu_z > .h_z. \end{aligned} \tag{AIII-3}$$

One writes the elements of the tensor (13) according to (AIII-1)–(AIII-3).

REFERENCES

[1] G. T. Rado, "Theory of the microwave permeability tensor and Faraday effect in nonsaturated ferromagnetic materials," *Phys. Rev.*, vol. 89, pp. 529, 1953.

[2] E. Schlömann, "Microwave behavior of partially magnetized ferrites," *J. Appl. Phys.*, vol. 41, no. 1, Jan. 1970.

[3] J. Green and F. Sandy, "Microwave characterization of partially magnetized ferrites," *IEEE Trans. Microwave Theory Tech.*, vol. MTT-22, pp. 641–645, June 1974.

[4] M. Igarashi and Y. Naito, "Tensor permeability of partially magnetized ferrites," *IEEE Trans. Magn.* vol. MAG-13, Sept. 1977.

[5] ——, "Parallel component μz of partially magnetized microwave ferrites," *IEEE Trans. Microwave Theory Tech.*, vol. MTT-29, pp. 568-571, June 1981.

[6] D. Polder and J. Smit, "Resonance phenomena in ferrites," *Rev. Mod. Phys.*, vol. 25, pp. 89–90, Jan. 1953.

[7] T. L. Gilbert "A Lagrangian formulation of the gyromagnetic equation of the magnetization field," *Phys. Rev.*, vol. 100, pp. 1243-1255.

[8] D. Polder, "On the theory of ferromagnetic resonance," *Philos. Mag.*, pp. 99–115, Jan. 1949.

[9] J. Green, F. Sandy, and C. Patton, "Microwave properties of partially magnetized ferrites," Raytheon Res. Div., Waltham, MA, Rep. RADC-TR-68-312, Aug. 1968.

[10] F. Liorzou, A. M. Konn, M. Le Floc'h, "A common expression for both direct and inverse magnetization curves in soft ferrites," *J. Magnetism Magn. Materials*, vol. A-12, pp. 140-144, Aug. 1995.

[11] S. Chikazumi, *Physics of Magnetism*. New York: Wiley, 1964

Philippe Gelin (A'87) was born in France in 1948. He received the Ph.D. degree in physics from the University of Lille, Lille, France, in 1981.

He is currently a Professor of electrical engineering at the Ecole Nationale Supérieure des Télé communications de Bretagne (Telecom Bretagne), Brest, France. His research interests include wave-matter interactions and the modeling and the characterization of materials.

Dr. Gelin is a member of the Laboratory for Electronics and Communication Systems (LEST), which is a research unit associated with the French National Research Council (UMR CNRS no. 6616).

Karine Berthou-Pichavant was born in France in 1969. She received both the B.S. degree and the B.S. degree (honors) in physics, the M.Sc. degree in electronics, and the Ph.D. degree in electronics, from the University of Brest, Brest, France, in 1991, 1992, 1993, and 1996, respectively.

In 1993, she joined the Laboratory for Electronics and Communication Systems (LEST), Brest, France. Her research interests include the modeling of non-saturated ferrites applied to microwave engineering.